A

Male Sprague-Dawley rats

160 chemicals
3 doses
8 time points

Collected tissues

Physiology
- hematology
- biochemistry
- body & organ weights

Histopathology

Transcriptome

 # samples   3,564   3,564   Liver – 3,528
Kidney – 975

B

1. Disease state identification

Physiology
① Normalization
② tSNE plot (physiology map)

Histology
③ Trimming observations
④ Mapping on physiology map
⑤ Imputing the observations

⑥ Identifying disease states

Dynamic analysis of DS
⑨ Transitions between disease states

2. Disease state characterization

Transcriptome
⑦ Normalization (Batch RMA)

⑧ Pathway analysis across multiple disease states

3. Mechanistic understanding of body weight loss
⑩ Integrative analysis of physiology, food consumption and transcritpome data.

C

Category	Class	Subclass	Target	Structure
Drugs (99)	CNS (27)	anticonvulsant (9)	GABAA agonist (5)	benzodiazepine (2)
		antidipressant (8)	serotonin inh (6)	SNRI, tricyclics (4)
		antipsychotic (6)	D2 inh (6)	phenothiazine (4)
	metabolic disease (25)	diabetes (6)	SUR1 inh (3)	sulfonylurea (3)
		lipid-lowering (6)	PPARA agonist (5)	fibrate (4)
		gastric secretion inh (4)	H2 inh (4)	
		uricosuric (3)	XO inh (3)	
		diuretic (3)		
	antiinflammatory, COXs (19)	NSAID (13)	COXs inh (11)	acetic acid (4)
				oxicam (3)
				propionic acid (2)
			COX2 inh (2)	
	circulatory (17)	antiarrythmic (7)	VNaCh inh (5)	alkaloid (2)
		hypotensive (4)	ACE inh (2)	
		vasodilator (4)	CaCh inh (4)	
		antianginal (3)		
		antispasmodic (2)		
	antiinflammatory, allergy (14)	antihistamine (14)	H1 inh (7)	
			H2 inh (4)	
		anti-rheumatic (4)		
	hormone (8)	androgen (2)	AR	
		antithyroid (2)	thyroid peroxidase inh (2)	
		estrogen (2)	ER	
		muscle relaxant (2)		
	PNS (2)			
Toxins (55)	toxin (27)	livertox (9)	DNA inh (4)	nitroso compound (4)
				nitroso compound, nitrosourea (2)
		alcohol (2)		
	antimicrobial (19)	antibacterial (14)		
		antibiotic (8)		
		antifungal (5)	fungal ergosterol synthesis inh (2)	
		tubercurosis (4)		
		synthetic antibacterial (2)		
	anticancer (13)		DNA inh (3)	containing Pt (2)
Endogenous (6)	endogenous (6)	vitamin (2)		

Figure S1, related to Figure 1. Experimental and analytical workflow in this study

(A) Experimental flow in Open TG-GATEs. (B) Analytical workflow in this study. (C) Known biological activity of 160 compounds investigated *in vivo* in Open TG-GATEs. Only the features shared by more than one compound are shown.

A

measurement	description	description	used
RBC	red blood cell count		y
Hb	hemoglobin		n
Ht	hematocrit value		n
MCV	mean corpuscular volume	MCH*RBC	y
MCH	mean corpuscular hemoglobin	MCV*RBC	y
MCHC	mean corpuscular hemoglobin concentration	MCH/MCV	n
Ret	reticulocyte		y
Plat	platelet count		y
WBC	white blood cell count		y
Neu	neutrophil		y
Eos	eosinophil		y
Bas	basophil	bad quality	n
Mono	monocyte		y
Lym	lymphocyte		y
PT	prothrombin time		y
APTT	activated partial thromboplastin time		y
Fbg	fibrinogen		y
ALP	alkaline phosphatase		y
TC	total cholesterol		y
TG	triglyceride		y
PL	phospholipid		y
TBIL	total bilirubin		y
DBIL	direct bilirubin		y
GLC	glucose		y
TP	total protein		y
RALB	albumin		y
A/G	albumin globulin ratio		y
AST	aspartate aminotransferase		y
ALT	alanine aminotransferase		y
LDH	lactate dehydrogenase		y
GGT	γ-glutamyltranspeptidase		y
BUN	blood urea nitrogen		y
CRE	creatinine		y
Na	sodium		y
K	potassium		y
Cl	chlorine		y
Ca	calcium		y
IP	inorganic phosphorus		y
Body.W	Body Weight		y
Liver.W	Liver Weight		n
Rel.Liver.W	Relative Liver Weight	Rel.Liver.W*Body.W	y
Kidney.W	Kidney Weight		n
Rel.Kidney.W	Relative Kidney Weight	Rel.Kidney.W*Body.W	y
Kidney.Right.W	Kidney Right Weight		n
Rel.Kidney.Right.W	Relative Kidney Right Weight	Rel.Kidney.Right.W*Body.W	n
Kidney.Left.W	Kidney Left Weight	strongly correlated with Rel.Kidney.W	n
Rel.Kidney.Left.W	Relative Kidney Left Weight	Rel.Kidney.Left.W*Body.W	n
		strongly correlated with Rel.Kidney.W	

Figure S2, related to Figure 1. Physiological parameters and their correlations

(A) 47 physiological parameters measured in Open TG-GATEs. In a 'description' column, shown 8 parameters that are calculated from other parameters. 2 that are extremely well-correlated with other parameters. These 10 redundant parameters were removed for t-SNE analysis because they do not carry unique information and outweigh correlated parameters in further analysis. 37 used parameters for the analysis were marked as y in 'used' column. (**B**) Heatmap showing Spearmn correlation coefficients between physiological parameters across 3,564 conditions. **(C-F)** Scatter plots of four pairs of parameters across 3,564 samples. Note that a parameter of each treatment was normalized by first subtracting corresponding value of vehicle treatment, then divided by interquartile range (IQR) of all 3,564 conditions. **(C)** an example of strong positive correlation: Ht and Hb. **(D)** comparison of two liver injury markers, ALT and DBIL. **(E)** comparison of two kidney injury markers, BUN and CRE. **(F)** strong negative correlation between Neu and Lym.
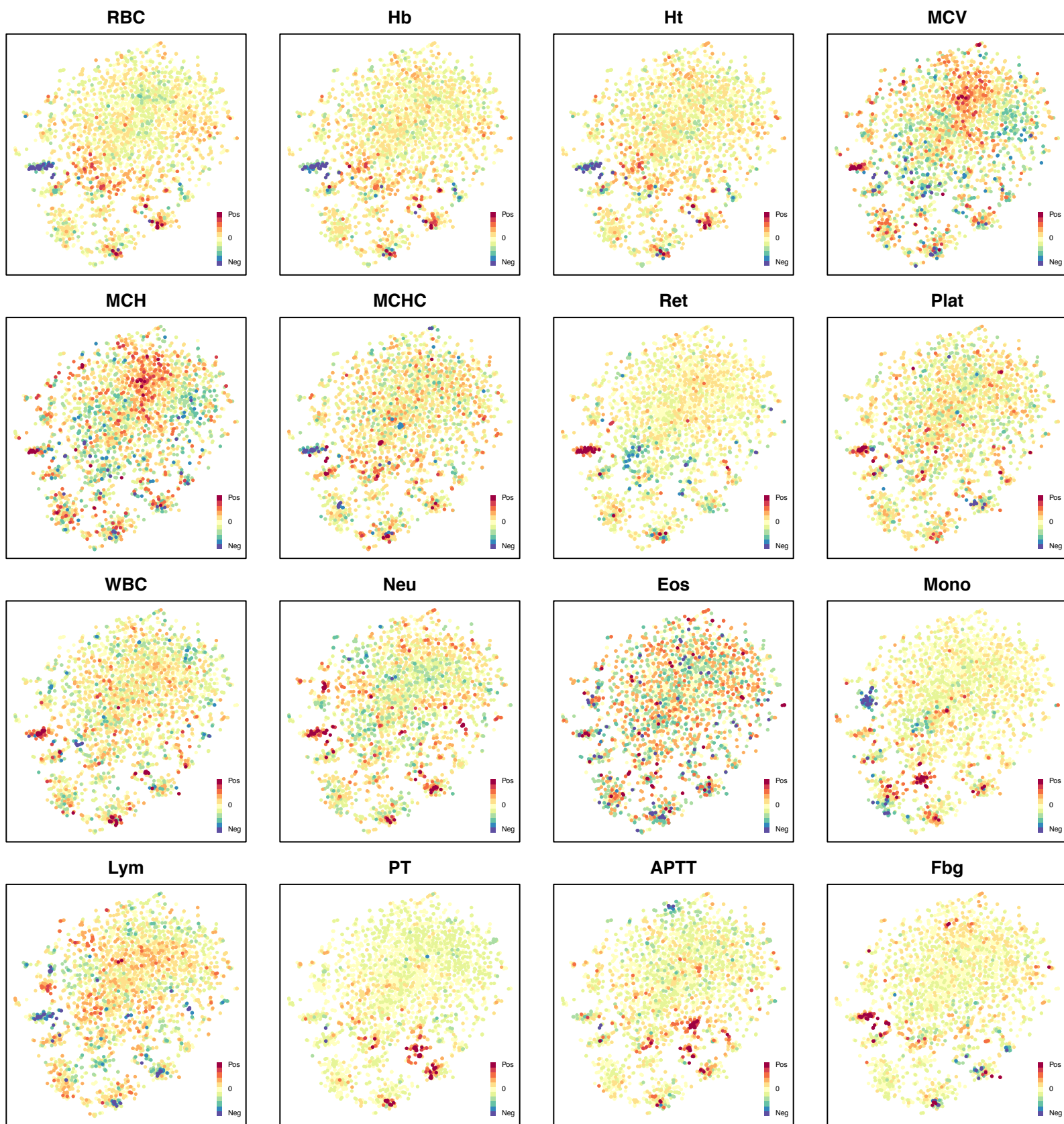
Figure S3, related to Figure 1. Physiology parameters on t-SNE map (1/3 page)
46 physiology parameters, as well as time point and relative doses (Low, Middle, High) of the measurements were mapped onto the physiology t-SNE map.
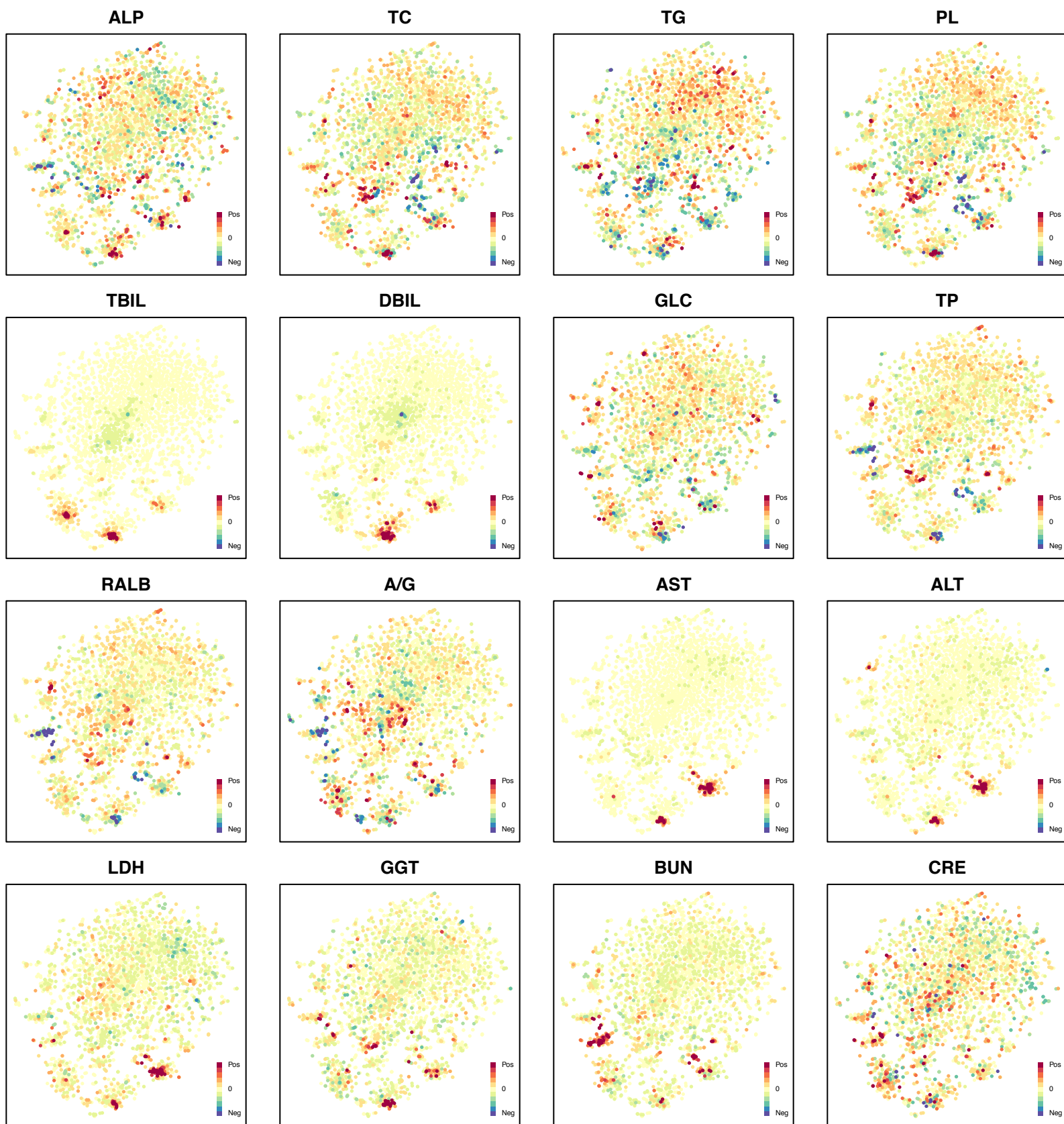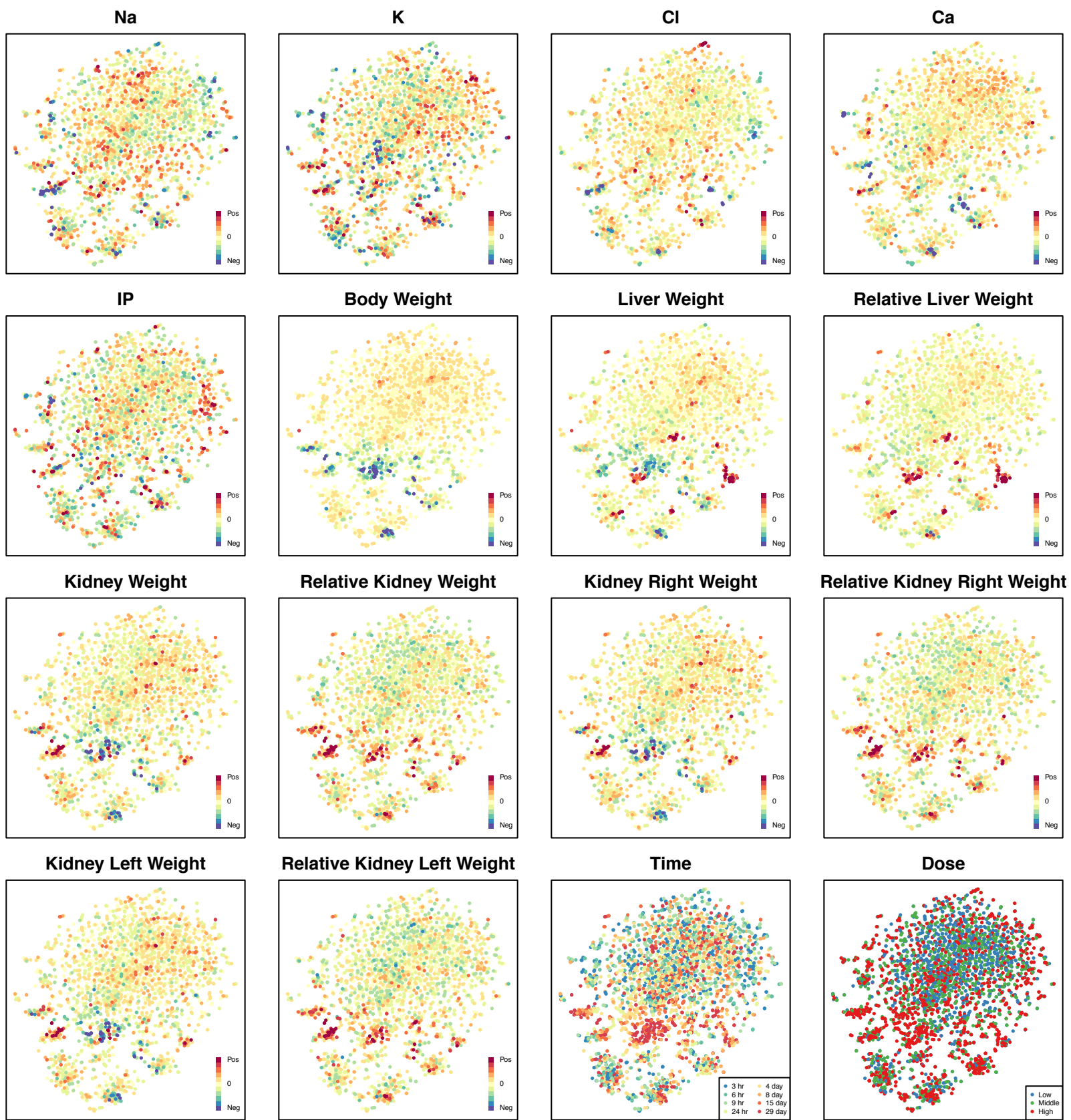
Figure S3, related to Figure 1. Physiology parameters on t-SNE map (continued, 2/3 page)
46 physiology parameters, as well as time point and relative doses (Low, Middle, High) of the measurements were mapped onto the physiology t-SNE map.

Figure S3, related to Figure 1. Physiology parameters on t-SNE map (continued, 3/3 page)
46 physiology parameters, as well as time point and relative doses (Low, Middle, High) of the measurements were mapped onto the physiology t-SNE map.
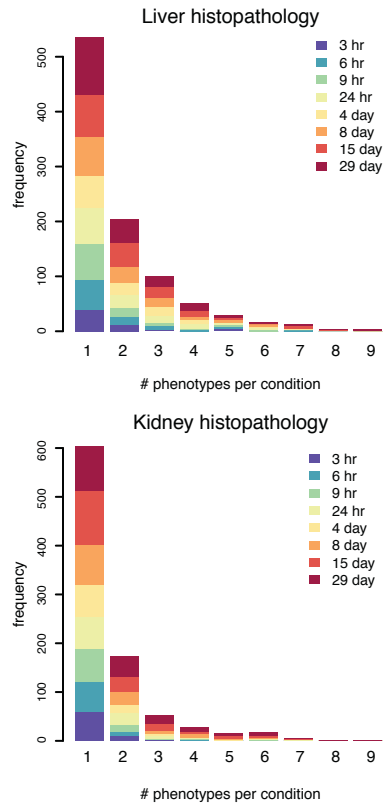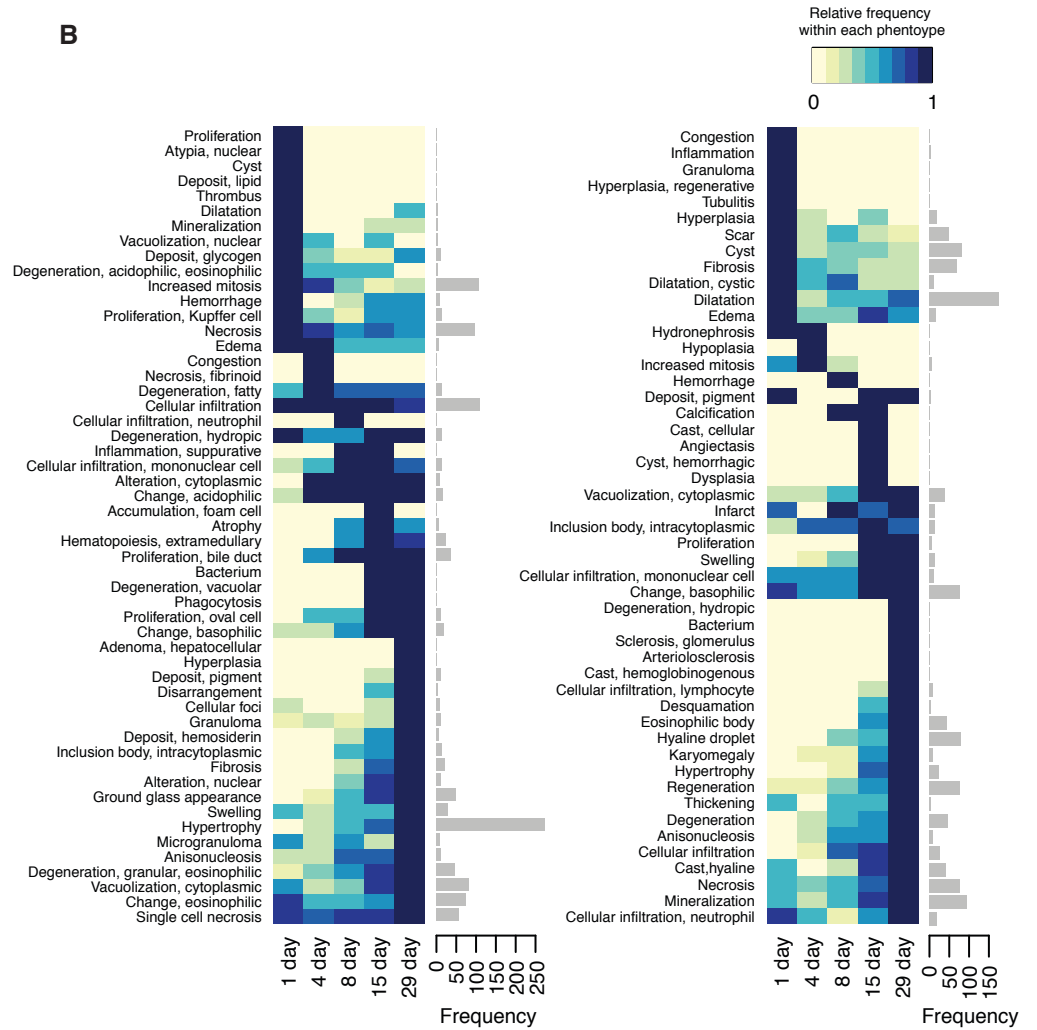
Figure S4, related to Figure 1. Kinetics of histopathology phenotypes
(A) Number of histopathology observations per condition, stratified by time points. **(B)** Kinetics of each histopathology phenotype. Color codes on the heatmap show relative frequency within each phenotype. Barplots on the right indicate the number of observations per each phenotype.

Figure S5, related to Figure 1. Histopathology mapped onto the physiology t-SNE (1/4 page)
Observations of each histopathology phenotypes in the liver (red) and kidney (blue) were mapped onto the physiology t-SNE plot.
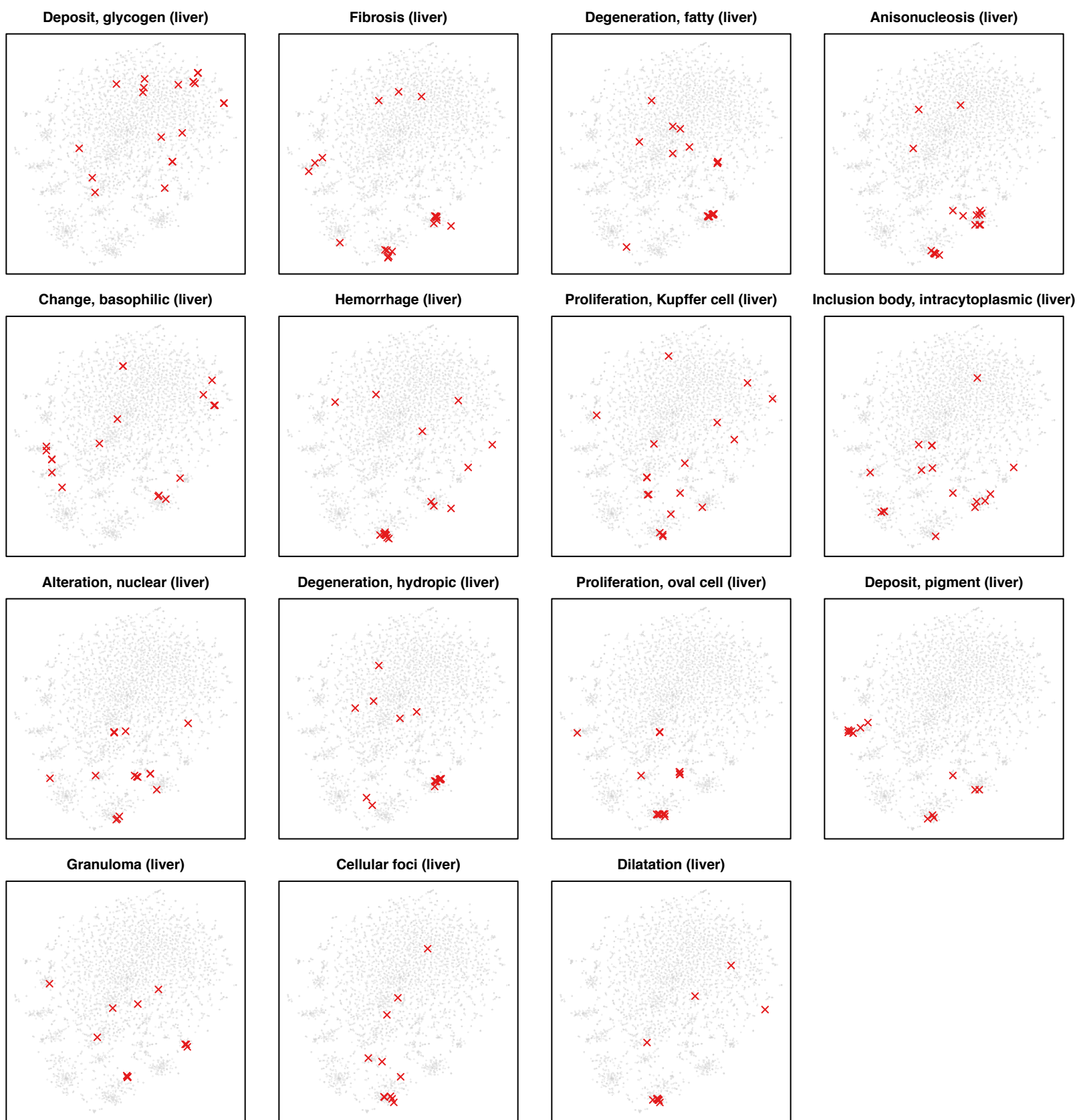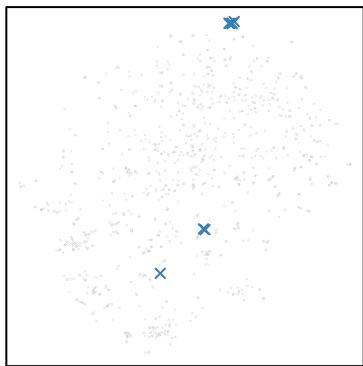
Figure S5, related to Figure 1. Histopathology mapped onto the physiology t-SNE (cont'd, 2/4 page)
Observations of each histopathology phenotypes in the liver (red) and kidney (blue) were mapped onto the physiology t-SNE plot.

Figure S5, related to Figure 1. Histopathology mapped onto the physiology t-SNE (cont'd, 3/4 page)
Observations of each histopathology phenotypes in the liver (red) and kidney (blue) were mapped onto the physiology t-SNE plot.

Cellular infiltration, neutrophil (kidney)
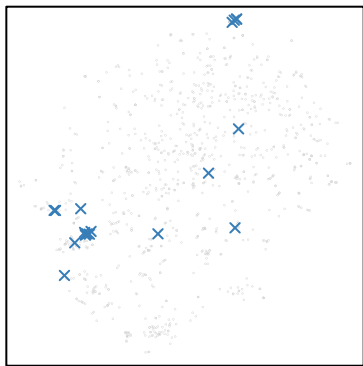
Edema (kidney)
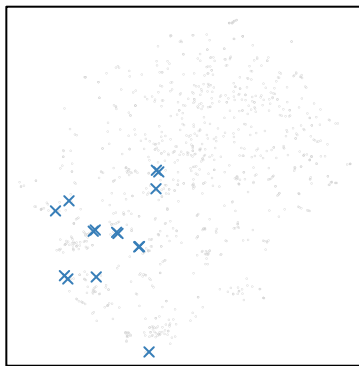
Infarct (kidney)
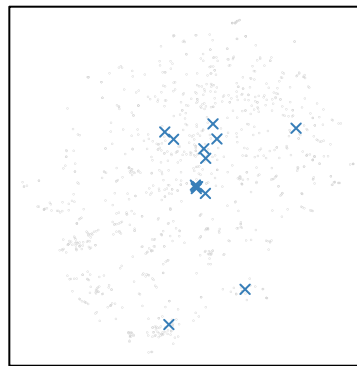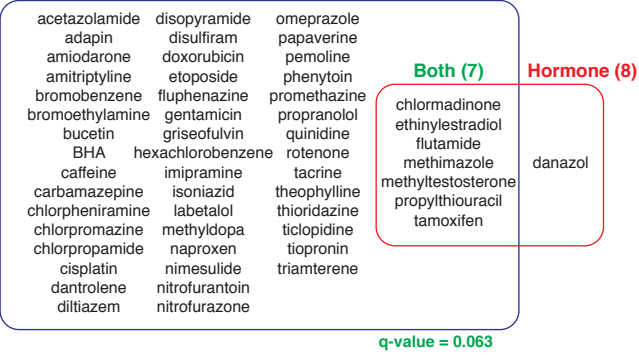
Swelling (kidney)
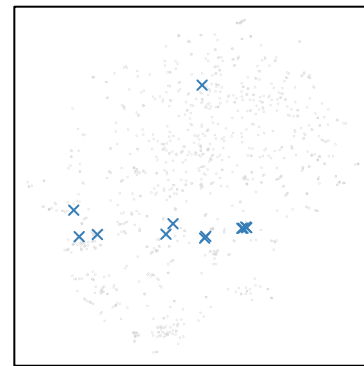
Dilatation, cystic (kidney)

Figure S5, related to Figure 1. Histopathology mapped onto the physiology t-SNE (cont'd, 4/4 page)
Observations of each histopathology phenotypes in the liver (red) and kidney (blue) were mapped onto the physiology t-SNE plot.
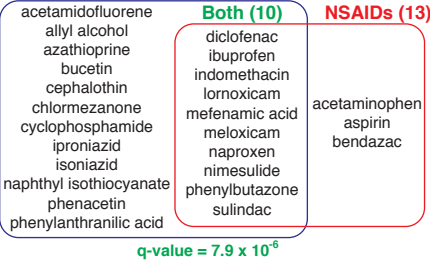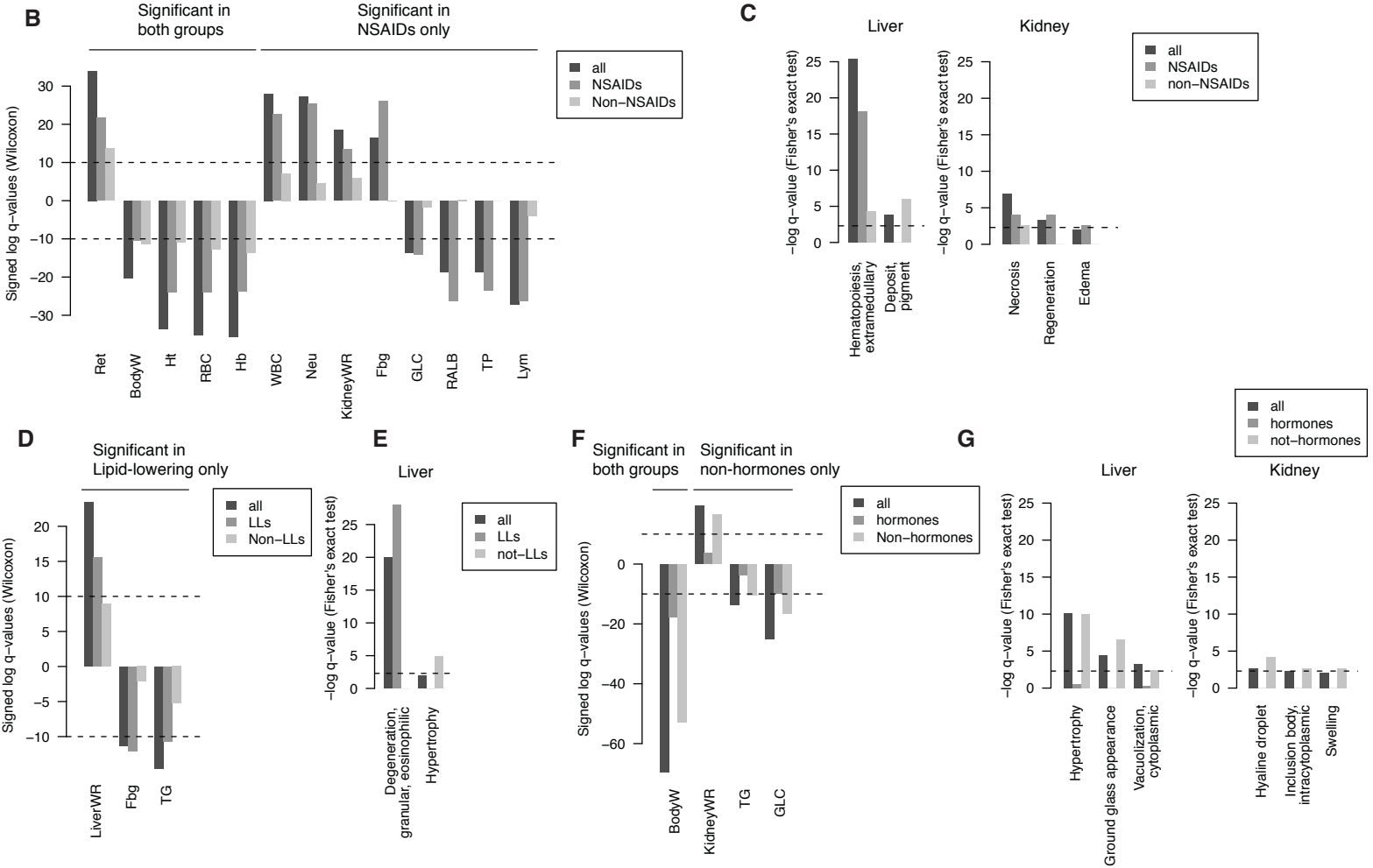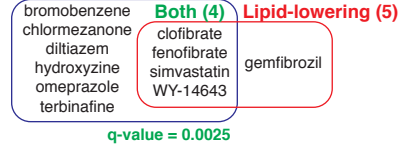
Figure S6, related to Table 1. Toxin class overrepresentations in DSs.

(A) Compound overrrepresentation in three DSs (q-value lower than 10^{-2}). **(B)** Changes in physiological parameters and of NSAIDs and non-NSAIDs in DS8. **(C)** Overrepresented histological phenotypes of NSAIDs and non-NSAIDs in DS8. **(D)** Changes in physiological parameters of lipid-lowering drugs and the other compounds in DS1. **(E)** Overrepresented histological phenotypes of lipid-lowering drugs and the other compounds in DS1. **(F)** Physiological changes of hormones and non-hormones in DS2. **(G)** Histopathological overrepresentation of hormones or non-hormones in DS2. For **B-G**, Thresholds for FDR-adjusted p-values (q-values) to call significant were set as 1×10^{-10} for physiology and 5×10^{-3} for histology.
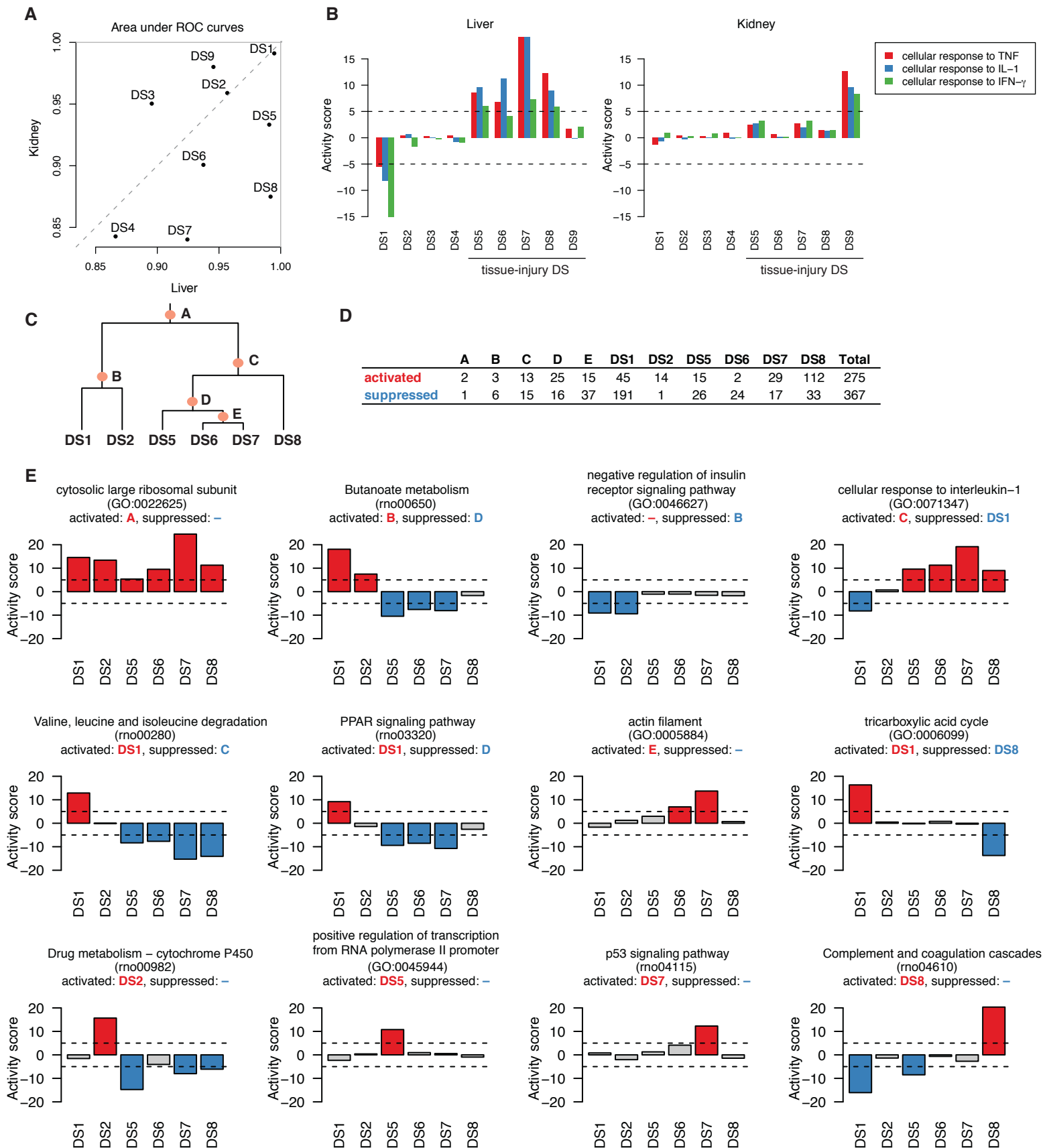
Figure S7, related to Figure 3. Transcriptome analysis for DS classification and kinetics

(A) Area under ROC curves from elastic net classifiers for each DS using either liver or kidney transcriptome data. **(B)** Transcriptional activity of GO terms 'cellular responses to individual proinflammatory cytokines (TNF, IFN-γ, IL-1)' against each DS. **(C)** Dendrogram of the six DSs which showed substantial liver transcriptome changes. Nodes A-E corresponds to multiple DSs. **(D)** Number of activated and suppressed pathways in each node (individual DS or multiple DSs). **(E)** Examples of 12 pathways and the corresponding nodes in which they were activated or suppressed. In some cases, such as suppression of rno00982 or rno04610, pathways were not assigned to any nodes because the pattern of activation/suppression did not uniquely match to any nodes.

A DS retention

Frequency of DS retention

acute, transient

chronic, stable

3 hr → 6 hr
6 hr → 9 hr
9 hr → 24 hr
24 hr → 4 day
4 day → 8 day
8 day → 15 day
15 day → 29 day
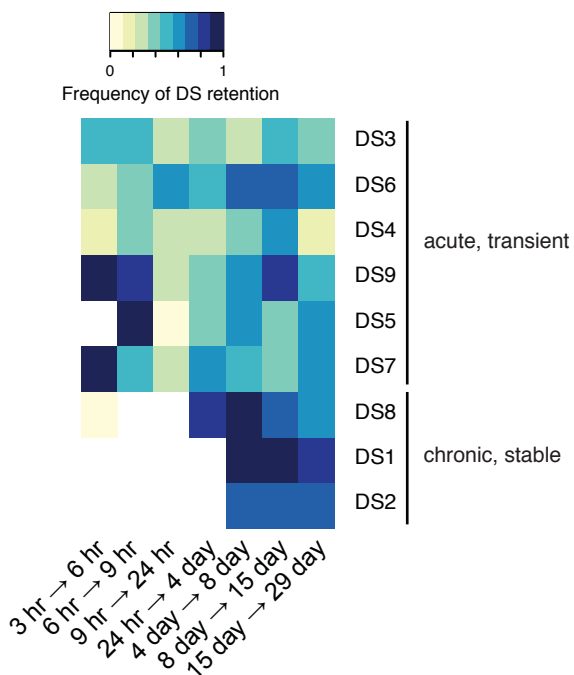
B # unique DS per condition

conditions (compounds x doses)

119 156 68 17 5

0 1 2 3 4

non-DS DS-experiencing
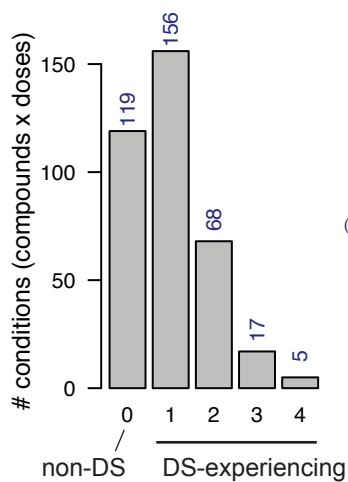
C DS transition centering DS2

DS5 (acute liver inj.)
DS4 (low TBIL)
DS6 (cholestasis)
DS3 (hemolysis)
DS7 (hepatocyte inj.)
DS2 (tolerance)
DS1 (active metab.)
DS8 (bleeding)
non–DS
DS9 (kidney inj.)
Dead

1 8 2
1 5 2 1
2 7
5 56

tissues affected
- liver
- kidney
- other inj.
- non–inflammatory
- dead

Figure S8, related to Figure 4. Disease state dynamics

(A) DS retention. A heatmap showing the ratio of conditions which retain the same DSs between two consecutive time points. **(B)** The number of unique DSs caused by one condition is summarized. **(C)** Same as DS transition graph in Fig. 4B except that this one highlights changes to and from DS2 only.
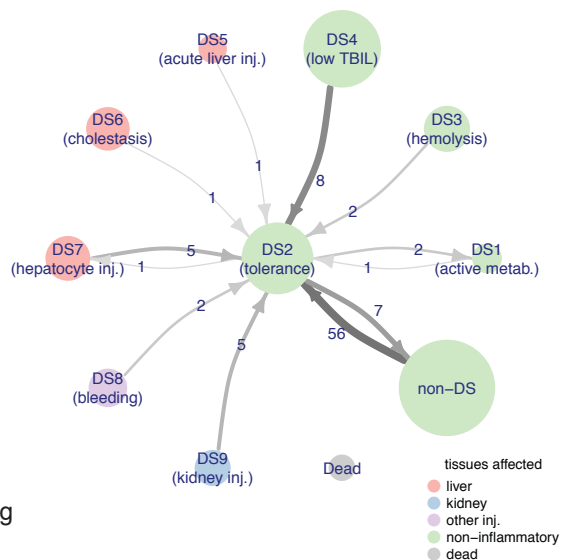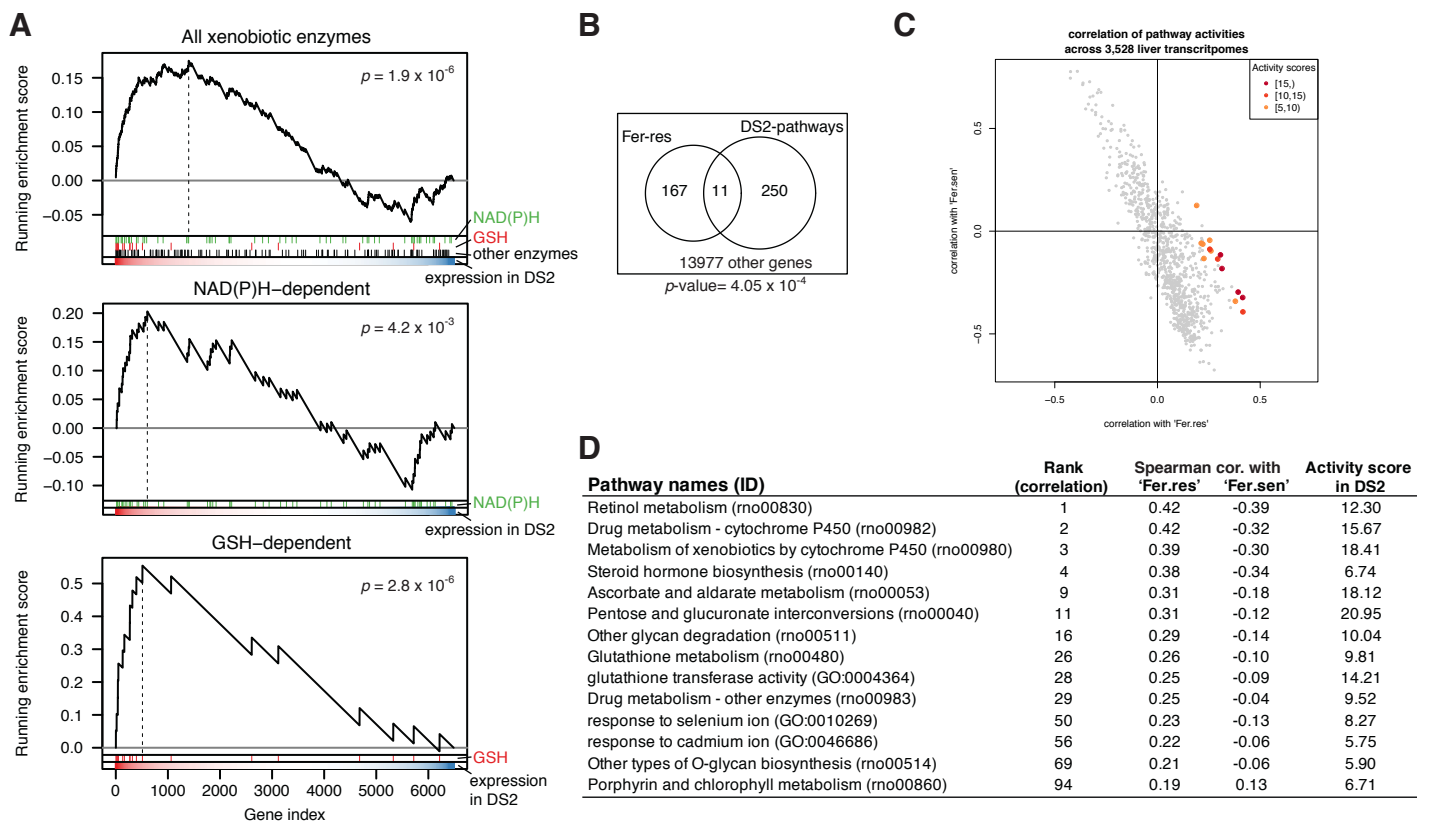
Figure S9, related to Figure 5. Induced drug tolerance is partly due to resistance to ferroptosis

(A) Enrichment of all drug metabolizing enzymes as well as NAD(P)H and GSH utilizng ones among activated genes in DS2. **(B)** Overlap between ferroptosis resistant signature and tolerance-associated pathways upregulated in DS2. p-value was calculated with one-sided Fisher's exact test. **(C)** Spearman correlation coefficients of pathway activities between 914 GO and KEGG pathways and Fer-sen or Fer-res. Red points correspond to the 14 pathways specifically upregulated in DS2 and their activity scores in DS2. Grey points corresponds to the other pathways. **(D)** Spearman correlation coefficients of the 14 DS2-specifically upregulated pathways against Fer-sen and Fer-res.

Pathway names (ID)	Rank (correlation)	Spearman cor. with 'Fer.res'	Spearman cor. with 'Fer.sen'	Activity score in DS2
Retinol metabolism (rno00830)	1	0.42	-0.39	12.30
Drug metabolism - cytochrome P450 (rno00982)	2	0.42	-0.32	15.67
Metabolism of xenobiotics by cytochrome P450 (rno00980)	3	0.39	-0.30	18.41
Steroid hormone biosynthesis (rno00140)	4	0.38	-0.34	6.74
Ascorbate and aldarate metabolism (rno00053)	9	0.31	-0.18	18.12
Pentose and glucuronate interconversions (rno00040)	11	0.31	-0.12	20.95
Other glycan degradation (rno00511)	16	0.29	-0.14	10.04
Glutathione metabolism (rno00480)	26	0.26	-0.10	9.81
glutathione transferase activity (GO:0004364)	28	0.25	-0.09	14.21
Drug metabolism - other enzymes (rno00983)	29	0.25	-0.04	9.52
response to selenium ion (GO:0010269)	50	0.23	-0.13	8.27
response to cadmium ion (GO:0046686)	56	0.22	-0.06	5.75
Other types of O-glycan biosynthesis (rno00514)	69	0.21	-0.06	5.90
Porphyrin and chlorophyll metabolism (rno00860)	94	0.19	0.13	6.71

A food consumption (grouped by DSs)

B food consumption and GLC

C correlation with food consumption per day

D Igf1 activity and body weight change (without synthetic hormones)

E with synthetic hormones
Latent variables (Igf1 activities):

		Estimate	Std.err	z-value	P(>|z|)
Liver	Igf1	1.000			
	Igfals	1.785	0.162	11.045	0.000
	Igfbp1	-4.315	0.512	-0.842	0.000
	Igfbp2	-3.164	0.342	-9.240	0.000
Kidney	Igf1	1.000			
	Igfals	0.714	0.232	3.070	0.002
	Igfbp1	-7.088	3.518	-2.015	0.044
	Igfbp2	0.281	0.113	2.486	0.013

F without synthetic hormones
Latent variables (Igf1 activities):

		Estimate	Std.err	z-value	P(>|z|)
Liver	Igf1	1.000			
	Igfals	2.202	0.210	10.498	0.000
	Igfbp1	-4.123	0.684	-6.024	0.000
	Igfbp2	-4.196	0.452	-9.276	0.000
Kidney	Igf1	1.000			
	Igfals	1.023	0.217	4.725	0.000
	Igfbp1	-2.357	0.449	-5.252	0.000
	Igfbp2	-0.305	0.112	-2.726	0.006

H Gdf15 expression and food consumption

Gdf15 expression vs food consumption

I Gdf15 expression vs food consumption

Gdf15 expression vs food consumption

J Tissue expression of Gdf15 and DSs

K Linear regression coefficients with symthetic hormone data

	tissue	Estimate	Std. Error	t value	Pr(>|t|)
All	liver	-2.31	0.22	-10.72	**3.72E-24**
	kidney	-2.28	0.29	-7.94	**1.51E-14**
tolerance	liver	-2.71	0.24	-11.52	**3.68E-27**
	kidney	-0.34	0.79	-0.43	6.64E-01
liver inj.	liver	-3.22	1.24	-2.60	9.55E-03
	kidney	-2.50	0.89	-2.81	5.16E-03
kidney inj.	liver	-4.73	1.91	-2.48	1.33E-02
	kidney	-3.77	0.57	-6.64	**8.68E-11**
bleeding	liver	-2.01	4.13	-0.49	6.27E-01
	kidney	-3.35	2.93	-1.14	2.53E-01
non injury	liver	-0.86	0.45	-1.90	5.86E-02
	kidney	-0.87	0.45	-1.95	5.19E-02

L Linear regression coefficients without symthetic hormone data

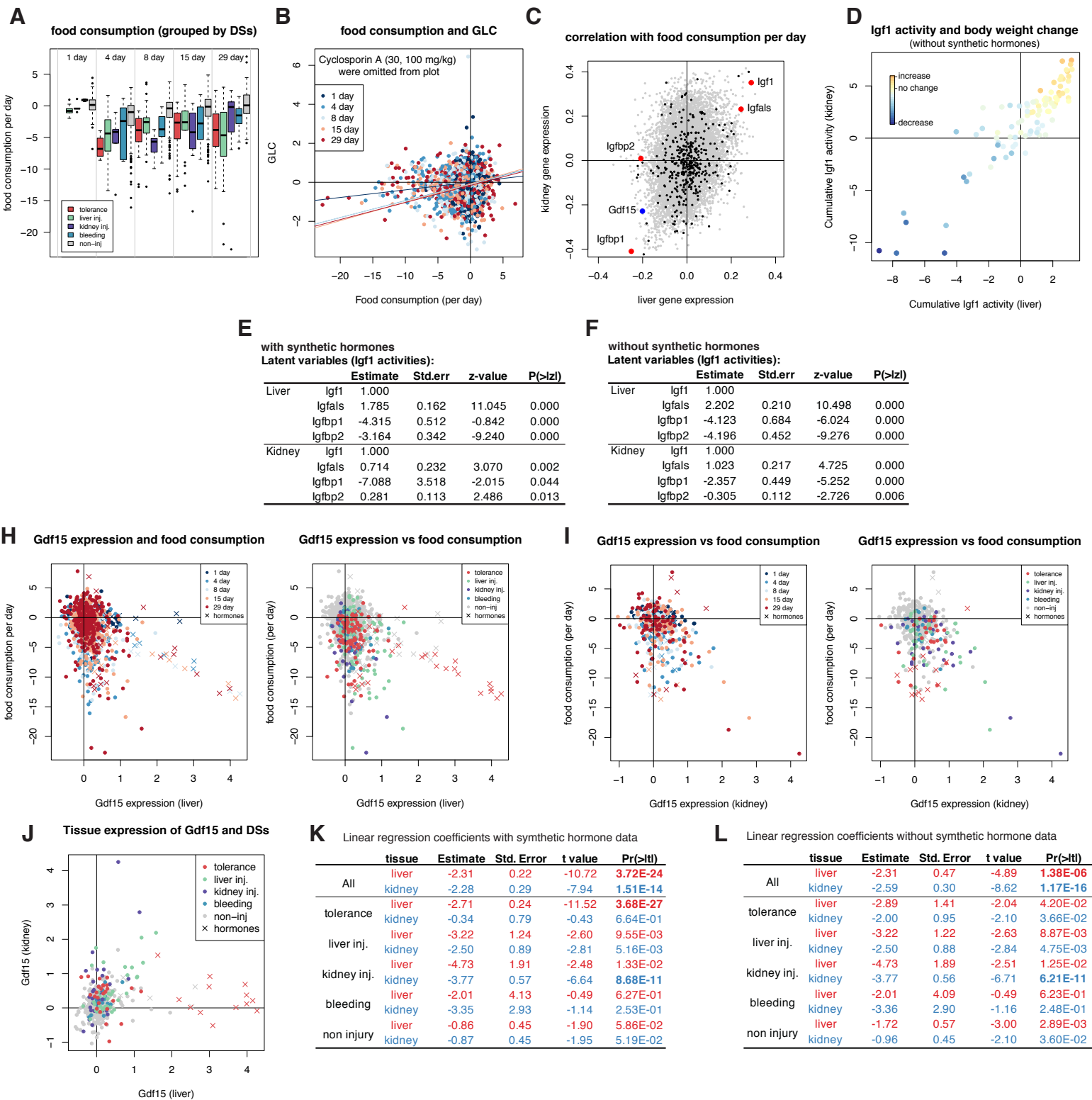|	tissue	Estimate	Std. Error	t value	Pr(>|t|)
All	liver	-2.31	0.47	-4.89	**1.38E-06**
	kidney	-2.59	0.30	-8.62	**1.17E-16**
tolerance	liver	-2.89	1.41	-2.04	4.20E-02
	kidney	-2.00	0.95	-2.10	3.66E-02
liver inj.	liver	-3.22	1.22	-2.63	8.87E-03
	kidney	-2.50	0.88	-2.84	4.75E-03
kidney inj.	liver	-4.73	1.89	-2.51	1.25E-02
	kidney	-3.77	0.56	-6.71	**6.21E-11**
bleeding	liver	-2.01	4.09	-0.49	6.23E-01
	kidney	-3.36	2.90	-1.16	2.48E-01
non injury	liver	-1.72	0.57	-3.00	2.89E-03
	kidney	-0.96	0.45	-2.10	3.60E-02

Figure S10, related to Figure 6. Mechanism of body weight loss
(A) Food consumption data were stratified by disease states at five time points. Note that no conditions took tolerance on Day 1. **(B)** Relationship between food consumption and blood glucose level (GLC). Linear regression on each time point were also plotted. Cyclosporine A treaments were omitted from the plots because they gave high GLC outliers, but they were used for linear regression computation. **(C)** Spearman correlations of each gene's expression with food consumption at five time points (1, 4, 8, 15, 29 days). Correlations were computed among 337 and 95 conditions (compounds and doses) in liver and kidney, respectively. **(D)** Cumulative Igf1 activity computed by using latent variable modeling. The modeling was performed in the same way as Fig. 6G but synthetic hormone treatments (6/91 treatments) were excluded. Points were color coded by body weight change on 29 day. **(E-F)** Contributions of four genes for computing Igf1 activity of corresponding tissues. The model was fit on the body weight and expression data **(E)** with or **(F)** without synthetic hormone data. **(H-I) (H)** liver or **(I)** kidney expression of Gdf15 and food consumption was plotted. Points were color coded by time points (left) and disease states (right). Conditions treated with synthetic hormones were marked by x (otherwise filled circles). **(J)** Gdf15's expression in liver and kidney are plotted. Points are color coded by disease states. Synthetic hormones are marked by x. **(K-L)** Summary of multivariate linear regresion of food consumption on liver and kidney Gdf15 expressions. Regression was computed using data **(K)** including synthetic hormone treatments, or **(L)** excluding them. In both, p-values lower than 10^{-5} were highlighted in bold letters.